NANO LETTERS

2007
Vol. 7, No. 10
3035−3040

Control of Curvature in Highly Compliant Probe Cantilevers during Carbon Nanotube Growth

I-Chen Chen,[†] Li-Han Chen,[†] Christine A. Orme,[‡] and Sungho Jin*[,†]

Materials Science and Engineering, University of California, San Diego, California 92093-0411, and Chemistry, Material and Life Science, Lawrence Livermore National Laboratory, 7000 East Avenue, Livermore, California 94550

Received June 22, 2007; Revised Manuscript Received September 5, 2007

ABSTRACT

Direct growth of a sharp carbon nanotube (CNT) probe on a very thin and highly flexible cantilever by plasma-enhanced chemical vapor deposition (PECVD) is desirable for atomic force microscopy (AFM) of nanoscale features on soft or fragile materials. Plasma-induced surface stresses in such fabrication processes, however, tend to cause serious bending of these cantilevers, which makes the CNT probe unsuitable for AFM measurements. Here, we report a new tunable CNT growth technique that controls cantilever bending during deposition, thereby enabling the creation of either flat or deliberately curved AFM cantilevers containing a CNT probe. By introducing hydrogen gas to the (acetylene + ammonia) feed gas during CNT growth and adjusting the ammonia to hydrogen flow ratio, the cantilever surface stress can be altered from compressive to tensile stress, and in doing so controlling the degree of cantilever bending. The CNT probes grown under these conditions have high aspect ratios and are robust. Contact-mode imaging has been demonstrated using these probe tips. Such CNT probes can be useful for bio-imaging involving DNA and other delicate biological features in a liquid environment.

The recent worldwide explosion of nanotechnology and nanobiotechnology research activities makes nanoscale atomic force microscopy (AFM) imaging an essential structural evaluation technique. Carbon nanotubes (CNTs) have attracted much attention as possible high-resolution AFM probe tips due to their high-aspect-ratio geometry and small diameter.[1−6] Although placing a single CNT probe on an AFM cantilever is generally not easy, several approaches have been reported for fabrication of CNT-based AFM probes. The earliest approaches used mechanical attachment of nanotubes onto an AFM pyramid. However this is time-consuming and it is difficult to reproduce the number, length, and angle of CNT placement. In addition, such tips are typically not viable in fluid environments. Direct chemical vapor deposition (CVD) growth of a single, vertically aligned CNT probe on AFM cantilever would be an attractive solution to this problem. By combining an electron beam lithography approach for catalyst patterning with plasma-enhanced CVD (PECVD) for CNT growth, the location, length, and diameter of CNTs can be readily controlled. A simpler and convenient technique for fabricating extremely sharp CNT probes using electron-beam-induced deposition of carbon island mask has recently been reported.[5,6]

For surface metrology of delicate surfaces of soft materials such as living cells, protein molecules, DNA, fragile cell membranes, or soft polymer nanostructures, low-stiffness AFM probe cantilevers with spring constants <0.1 N/m, which allow low imaging forces, is desirable to minimize structural damage during scanning. The plasma-induced stresses and damages introduced during PECVD growth of nanotubes, however, results in severely bent cantilevers when thin, low-stiffness cantilevers are utilized as a substrate. If the bend is sufficiently large, the AFM laser spot focused at their end will be deflected off of the position-sensitive detector, rendering the cantilevers unusable for AFM measurements.

An example of such an undesirable cantilever bending during CNT growth is shown in Figure 1. The probe system in the figure contains three 1 μm thick silicon cantilevers with different lengths. It is seen that all three CNT-containing cantilevers are significantly bent upward after PECVD growth of CNTs using a feed gas mixture of acetylene (C_2H_2) and ammonia (NH_3) gas, a commonly used recipe for CNT growth.[5−7]

In this work, we have developed a new in situ process to control the deflection of cantilever beams during the CNT growth stage. A single, sharp CNT has successfully been grown on a flat, low-stiffness cantilever (spring constant <0.1 N/m). In fact, this new control process utilizing a gas mixture

* To whom correspondence should be addressed. E-mail: jin@ucsd.edu.
[†] University of California, San Diego.
[‡] Lawrence Livermore National Laboratory.

10.1021/nl071490x CCC: $37.00
Published on Web 09/22/2007

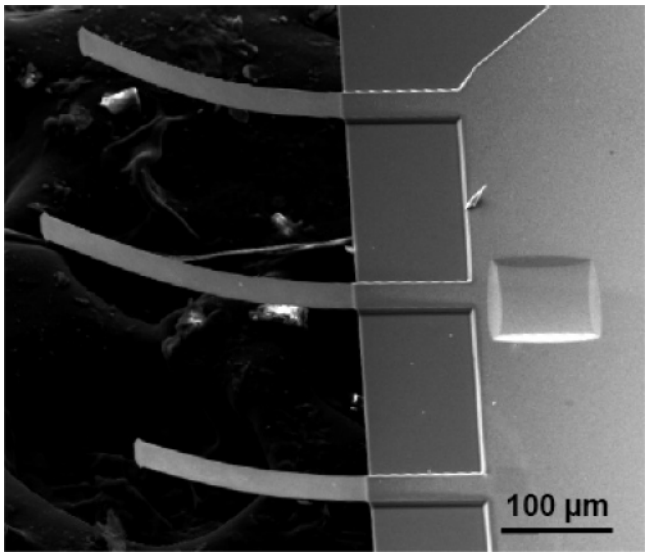

Figure 1. SEM image of bent cantilevers after PECVD growth of carbon nanotubes.

composition allows the fabrication of CNT probes with an intentional and programmable cantilever curvature if desired. Contact-mode imaging was performed with a flat-cantilever CNT probe so fabricated.

The experimental procedures used for fabrication of CNT-based AFM probes on low-stiffness cantilevers are described as follows. A ~10 nm thick Ni catalyst film was deposited on Si tipless cantilever chips (CSC12/Tipless, MikroMasch USA) using an electron beam evaporator. The length of the selected cantilevers was ~350 μm. The spring constant was ~0.03 N/m, about 3 orders of magnitude more compliant than the standard tapping-mode AFM probes. For growth of a single CNT, the patterning of a single catalyst island was made using electron-beam-induced deposition (EBID) of a carbon dot, which served as an etch mask. After wet etching of unmasked Ni and removal of the carbon dot mask from the surface by oxygen plasma etching, a Ni catalyst island of 200 nm diameter was obtained.[6] The low-stiffness Si cantilever with the Ni dot was then placed into the DC PECVD system and heated up to 700 °C for electric-field-guided growth of a CNT.[5−7] The growth was carried out using a feed gas mixture of H_2, NH_3, and C_2H_2 gas at 2−5 mtorr pressure. The total flow rate of NH_3 and H_2 was kept constant during growth, while the gas mix ratio (R) defined as $NH_3/(NH_3 + H_2)$ was varied in the range $0 \leq R \leq 1$. For the characterization, optical microscopy (OM) and scanning electron microscopy (SEM) were used to examine the cantilever deflection (bending) and CNT probe geometry. The magnitudes of deflections at the free ends of the cantilevers were measured by an optical profiler (Veeco Wyko NT1100). Probe performance was evaluated in contact mode using a Dimension 3100 AFM with Nanoscope IIIa controller (Veeco Instruments) in air. To identify the change of surface chemistry of the plasma-treated cantilevers, Fourier transform infrared spectroscopy (FTIR) spectra analysis was carried out using a Nicolet Magna 550 spectrometer, and the base signal of a non plasma-treated silicon spectrum was subtracted from the data. Samples with a 1 cm × 1 cm area with various plasma treatment conditions were used for FTIR analysis.

The bending of low-stiffness cantilevers during CNT probe fabrication is attributed to the change in surface stresses introduced during the PECVD process. Surface stresses have been investigated for many years, and they are known to be associated with ion-assisted fabrication processes such as ion implantation,[8] reactive ion etching,[9] and PECVD growth of thin films.[10] The surface stress is often caused by strains at film interfaces, from surface disorder, surface reconstruction, or bonding configuration.[11] A number of experiments have shown that the profile of low-energy (<1 KeV) ion-induced damage can extend tens or even hundreds of times deeper than the nominal ion penetration range for the given acceleration energy (within ~5 nm for most of ions) predicted by Monte Carlo simulation techniques.[12−14] The primary mechanisms for extended defect profiles are radiation enhanced diffusion[13] and channeling.[14] Thus, the $NH_3-C_2H_2$ mixed plasma, which was turned on with 500 V dc bias, is expected to interact with or induce damages on the Si substrate, especially at the relatively high CNT growth temperature of 700 °C, which can enhance thermal diffusion of ions and interaction rate with Si substrate.

Shown in Figure 2 are comparative, cross-sectional cantilever images for three different CNT growth conditions using different feed gas composition. Figure 2a shows the cantilever bending after 10 min PECVD growth of CNTs using NH_3 and C_2H_2 gases at flow ratio 6:1. It is seen from Figure 2a that the surface stress on the top surface of the cantilever is tensile[15] and the upward bending deflection in the cantilever is huge (as much as 120 μm), almost a third of the cantilever length of ~350 μm. In the FTIR spectrum of the sample after $NH_3-C_2H_2$ ($R = 1$) plasma growth of CNTs, Figure 3a, a large peak is seen near 840 cm^{-1}, which is attributed to the vibrations of the Si−N stretching bonds. The large deflection of the cantilever is most likely caused by ion-induced modification of the Si subsurface, which can form a defect layer dominated by nitrogen species. From the measurement of secondary ion mass spectroscopy (SIMS) on the plasma-treated sample (data not shown here), we observe that nitrogen atoms diffuse into the Si substrate by more than 50 nm. It has been reported that NH_3 plasmas were used for nitridation of silicon.[16,17] The growth rate of silicon nitride (Si_3N_4) is very slow (~5.5 nm/hr with RF power at a higher temperature of 950 °C) because of high density of Si_3N_4 layer.[17] In our case, however, plasma damage may be more dominant because a high bias voltage was directly applied to the substrate, which differs from refs 16 and 17. Thus, it is likely that both plasma damage (lattice defect layer) and perhaps some surface reconstruction (nonstoichoimetric nitride formation) contribute to the induced stress in our samples. The Si−C bands at 790 cm^{-1} in the FTIR spectrum of Figure 3 is not obvious because the formation of SiC requires a higher temperature with longer annealing time. In addition, NH_3 plasmas can etch away carbohydrate radicals adsorbed on the substrate surface and reduce the interaction between the surface and radicals.

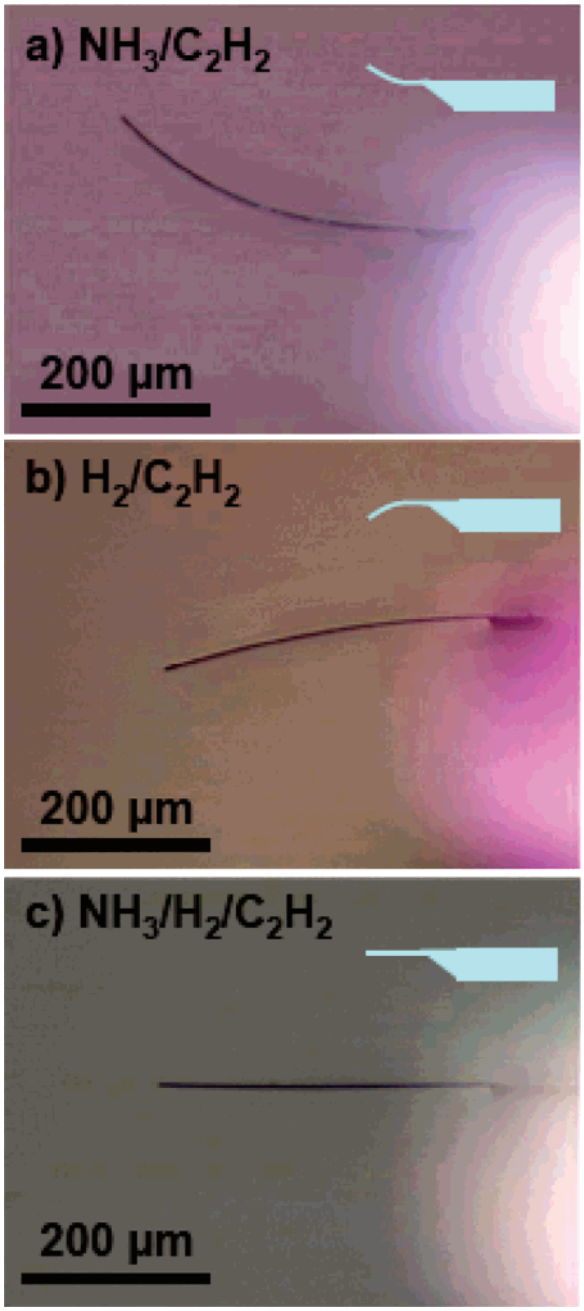

Figure 2. Optical microscope images of cantilevers after plasma treatments with C_2H_2 gas and (a) NH_3 gas ($R = 1$). (b) H_2 gas ($R = 0$). (c) Mixed NH_3-H_2 ($R = 0.5$).

Therefore, nitrogen-related damage during CNT growth from the presence of NH_3 feed gas is considered to have a more pronounced effect on the cantilever bending than the C_2H_2 component of the feed gas.

To balance the undesirable tensile surface stress of the Si cantilevers induced by $NH_3-C_2H_2$ plasma, we employed an approach of introducing another type of gas that could induce a stress with an opposite sign (i.e., compressive stress) and yet still enable the CNT growth with desirable configuration. The SiO_2 film grown by thermal oxidation on Si wafers[18] as well as by oxygen plasma oxidation[19] has been observed to induce a compressive stress. Although oxygen plasma can induce compressive stress to compensate the undesirable

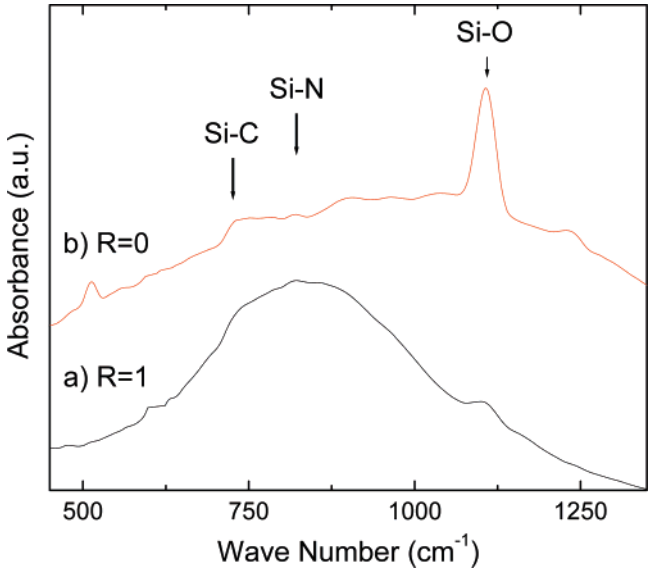

Figure 3. FTIR spectra of the silicon substrate. (a) After plasma treatment with C_2H_2 and NH_3 gas ($R = 1$). (b) After plasma treatment with C_2H_2 and NH_3 gas ($R = 0$).

tensile stress caused by NH_3 plasma, it is not desirable for use in our case because of undesirable oxidative etching of CNTs.

The next choice of gas to be employed in our CNT growth system was hydrogen. It has been reported that a thin SiO_2 layer can still be formed after hydrogen plasma treatment of porous silicon substrate due to the residual oxygen in the plasma system.[20] It has also been reported that hydrogen implantation may enhance oxygen accumulation at the buried layer,[21] which may induce compressive stress. As hydrogen can be used as a carrier gas for PECVD growth of CNTs, we attempted to apply plasma treatment on the low-stiffness Si cantilever using mixed $H_2-C_2H_2$ gases. The results of this experiment indicate that the $H_2-C_2H_2$ plasma treatment indeed introduces a compressive stress, thus enabling the downward bending of the cantilever during CNT growth as shown in Figure 2b. From the FTIR spectrum, Figure 3, curve b, the peak at 1107 cm^{-1} becomes much stronger, which is attributed to interstitial Si−O−Si asymmetric stretch mode with oxygen in interstitial sites of bulk Si. However, there is no obvious Si−O−Si stretching band corresponding to SiO_2 (around 1070 cm^{-1}), which implies that SiO_2 was not quite formed during our plasma treatment. Hence, the observed downward bending Si cantilever is likely caused by interstitial oxygen after the $H_2-C_2H_2$ plasma treatment. Such interstitial oxygen can put surrounding Si lattice under a compressive stress.[22] It is speculated that the source of oxygen in our PECVD system is most likely from the residual oxygen because the base pressure in the CVD chamber is not very low. The possible reason for no observed SiO_2 is that plasma oxidation from the residual oxygen may be counterbalanced by the reduction reaction in the hydrogen plasma. Further research is needed to elucidate the exact mechanism of surface stress during the plasma treatments.

To determine whether the C_2H_2 gas used for CNT growth has any effect on the surface stresses and cantilever bending,

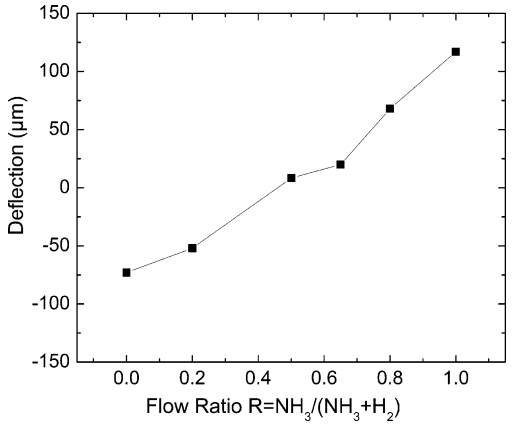

Figure 4. Magnitude of the cantilever deflection vs NH_3-H_2 flow ratio R during nanotube growth.

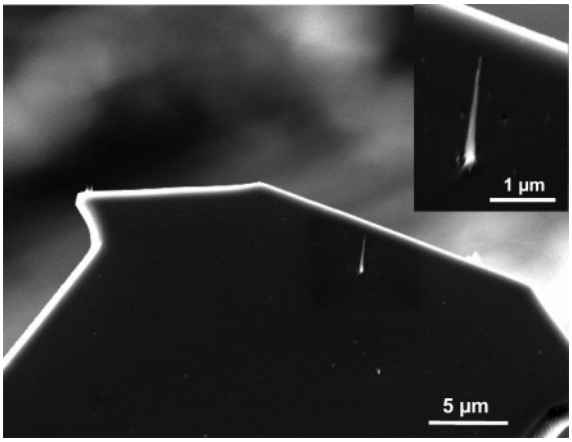

Figure 5. SEM image of a single CNT probe grown near the edge of a low-stiffness cantilever (45° tilted view). Inset: higher-magnification image of the CNT probe.

plasma experiments at the identical temperature but without C_2H_2 gas were carried out. The results indicate that a similar level of cantilever bending is obtained without using C_2H_2 gas, which implies NH_3 and H_2 are the main controlling factors that influence the surface stress of the cantilever. Thus, by adjusting the NH_3-H_2 flow ratio, different bending profiles of a cantilever were obtained. By employing a particular gas ratio of $R = 0.5$, a nearly flat cantilever beam can be obtained after PECVD growth of a CNT probe, as shown in Figure 2c.

The bending of the cantilevers after the plasma processing has been studied as a function of NH3/H2 flow ratio (Figure 4). The positive deflection represents the cantilever surface under tensile stress. By decreasing the gas flow ratio R, the stress condition is changed from tensile to compressive stress. For $R = 1$ (only NH3 and C_2H_2), a large upward bending of $\sim$120 μm is obtained, while for $R = 0$ (only H_2 and C_2H_2), a large downward bending of $\sim$70 μm is observed as shown in Figure 4. A stress-free cantilever with essentially flat geometry can be obtained within a window of R value between 0.45 and 0.55.

Figure 5 shows the SEM image of an AFM probe containing a single, high-aspect-ratio CNT probe grown on a tipless cantilever. The balanced feed gas ratio of $R \sim 0.5$

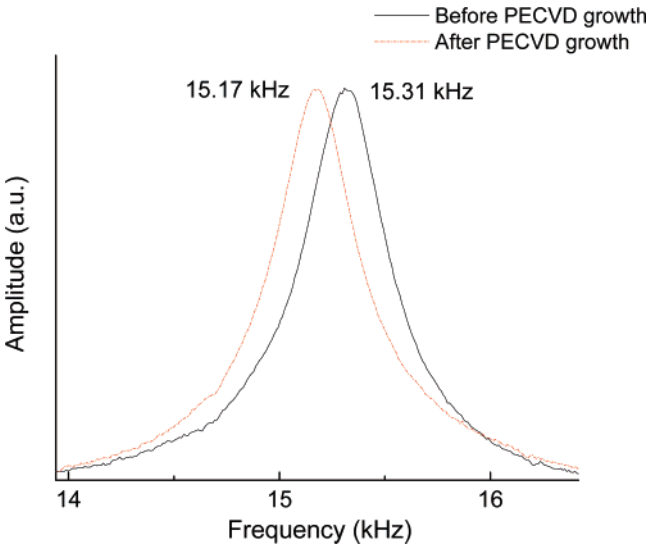

Figure 6. Resonance frequency of the low-stiffness cantilever before vs after PECVD growth of a CNT probe.

discussed above was utilized to avoid undesirable curvature and obtain a flat cantilever of Figure 2c. The inset in Figure 5 is a higher-magnification SEM micrograph (taken with 45° tilt) of the CNT tip. The height of the CNT was $\sim$2.5 μm, and the base diameter was $\sim$250 nm. The cone-shaped probe geometry is desirable, as the wider base provides mechanical rigidity and adhesion strength, while the much sharper tip produces high-resolution imaging without encountering the thermal vibration problem often seen in very thin diameter probes. It is well-known that the CNT diameter is dictated by the size of the catalyst particle at the tip. We accomplish the desirable nanocone geometry by gradually reducing the catalyst diameter during the CNT growth. When a dc bias voltage of higher than 550 V is applied in our DC-PECVD system, gradual plasma etching away of the catalyst particle occurs with gradually decreasing Ni catalyst diameter and, as a result, a conical CNT configuration instead of equi-diameter nanotube geometry is obtained.[5,6] The aspect ratio as well as the tip radius of the conical CNT can thus be controlled by adjusting the CVD growth conditions, especially by the magnitude of the bias voltage and the time of CVD growth.

Figure 6 shows the resonance frequency of the cantilever before and after PECVD growth of a CNT probe with flow ratio $R = 0.5$. The deviation of the resonance frequency is rather small, less than 1 kHz, which means the mechanical properties of the cantilever do not change much after PECVD growth using the $(NH_3 + H_2)$ mixed gas together with C_2H_2 gas. The small change in the resonance frequency might have been caused by the plasma-damaged layer or the slight increase in the cantilever mass after PECVD growth of CNTs.

The AFM imaging performance of the CNT probe in Figure 5 was evaluated in contact mode using a Dimension 3100 AFM with Nanoscope IIIa controller (Veeco Instruments). The surface morphology of a bovine serum albumin (BSA) film on a freshly cleaved mica surface (prepared by dipping freshly cleaved mica into 0.1% BSA solution in

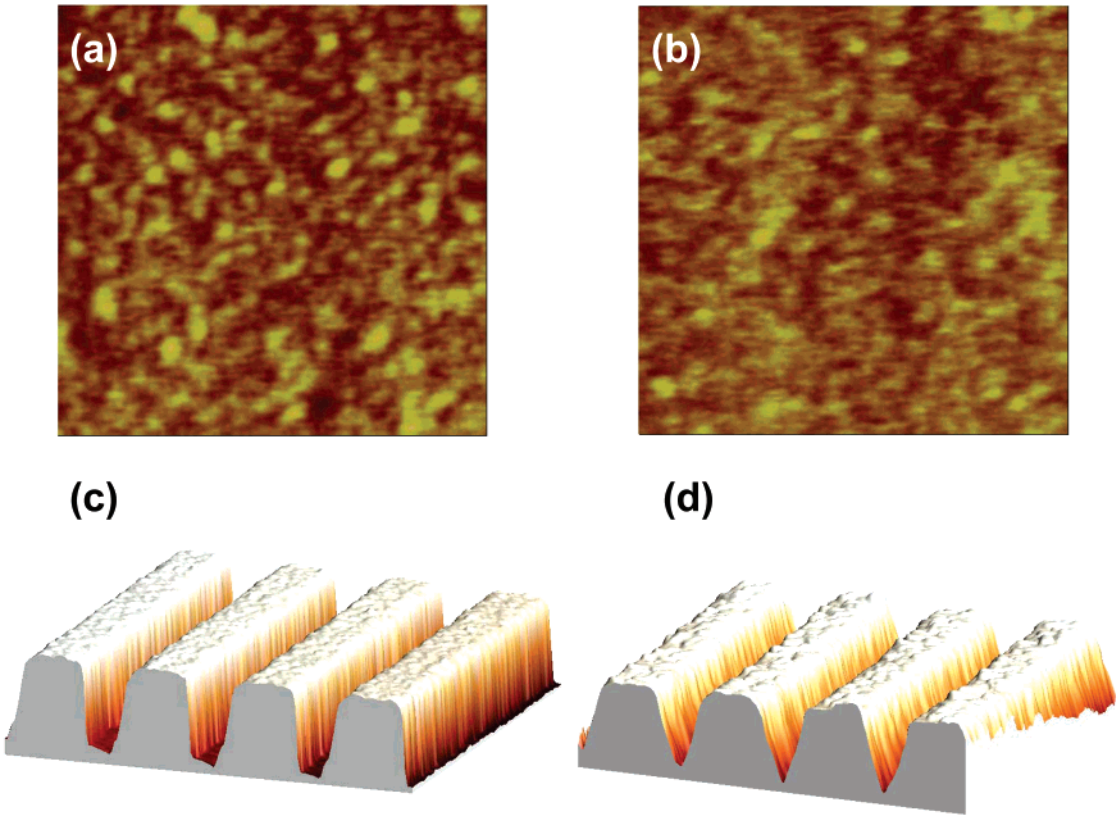

Figure 7. (a) AFM image (500 nm × 500 nm) of a bovine serum albumin (BSA) film by a CNT tip. (b) AFM image (500 nm × 500 nm) of the same BSA film by a commercial silicon nitride tip. (c) AFM image of a PMMA pattern by a CNT tip. (d) AFM image of the same PMMA pattern by a commercial silicon nitride tip.

phosphate buffered saline (PBS) for 20 min) was examined using our CNT probes and compared with the image taken by commercial silicon nitride contact-mode probes (NP series probes, Veeco), as shown in Figure 7a,b. As is evident from Figure 7a, the CNT probe produces a clearer image with better lateral resolution than the silicon nitride probe, Figure 7b. The improved image quality is revealed presumably due to the sharpness of the CNT tip and possibly its hydrophobic surface, which can reduce the capillary force during imaging and thus allow acquiring better images.

Another comparison between a CNT probe and a commercial silicon probe has been made by imaging an array of polymethyl methacrylate (PMMA) polymer resist pattern (600 nm trench line width, 250 nm spacing, and 350 nm thickness) on a Si substrate as shown in Figure 7c,d. Because of its high-aspect-ratio geometry, our CNT probe reveals more accurately the geometry of PMMA patterns. On the other hand, the silicon nitride probe shows misleading image due to the tip convolution of the pyramidal tip. As to the wear characteristics of CNT probes, we have shown the image quality, when operating in tapping mode, is not degraded after 7 h continuous scan on silicon nitride film, which implies that the CNT probe is very durable.[6] The durability of CNT probes operated in contact mode needs more experiments to test.

Obviously, the tip diameter will correlate to AFM imaging performance. The tip diameter of the conical CNTs grown by PECVD is generally in the range of <10 nm.[5,6] Further studies are needed to quantitatively compare the image quality to the sharpness of CNT probes on low-stiffness cantilevers.

In summary, we have demonstrated, for the first time, that a high-aspect-ratio CNT probe on a very compliant and low-stiffness AFM probe cantilever can be fabricated using a new controllable PECVD process of adjusting hydrogen/ammonia gas ratio in CNT growth and manipulating the surface stress conditions. Such a sharp nanotube probe on a highly flexible yet flat cantilever can be useful for enabling delicate AFM imaging applications for soft materials, especially for bio-imaging in liquid involving live cells, DNAs, and so forth. Contact-mode imaging of deep trench features has also been demonstrated using these CNT probes. By utilizing this tunable PECVD process of CNT growth, CNT probes can be fabricated with well-controlled geometry on flat nanoscale cantilevers for some possible applications such as biosensors.

Acknowledgment. We thank Dr. Robert E. Rudd's for useful discussions. This research was supported by NSF-NIRTs under grant numbers DMI-0210559 and DMI-0303790, University of California Discovery Fund under grant no. ele05-10241/Jin Lawrence Livermore National Lab (LLNL) MRI fund no. 04-006. Portions of this work were performed under the auspices of the U.S. Department of Energy by the University of California, Lawrence Livermore National Laboratory, under contract W-7405-Eng-4.

References

(1) Dai, H.; Hafner, J. H.; Rinzler, A. G.; Colbert, D. T.; Smalley, R. E. *Nature* **1996**, *384*, 147−150.
(2) Stevens, R.; Nguyen, C.; Cassell, A.; Delzeit, L.; Meyyappan, M.; Han, J. *Appl. Phys. Lett.* **2000**, *77*, 3453−3455.
(3) Yenilmez, E.; Wang, Q.; Chen, R. J.; Wang, D.; Dai, H. *Appl. Phys. Lett.* **2002**, *80*, 2225−2227.
(4) Ye, Q.; Cassell, A. M.; Liu, H. B.; Chao, K. J.; Han, J.; Meyyappan, M. *Nano Lett.* **2004**, *4*, 1301−1308.
(5) Chen, I.-C.; Chen, L.-H.; Ye, X.-R.; Daraio, C.; Jin, S.; Orme, C. A.; Quist, A.; Lal, R. *Appl. Phys. Lett.* **2006**, *88*, 153102/1−153102/3.
(6) Chen, I.-C.; Chen, L.-H.; Orme, C.; A.; Quist, A.; Lal, R.; Jin, S. *Nanotechnology* **2006**, *17*, 4322−4326.
(7) AuBuchon, J. F.; Chen, L. H.; Gapin, A. I.; Kim, D. W.; Daraio, C.; Jin, S. *Nano Lett.* **2004**, *4*, 1781−1784.
(8) Burnett, P. J.; Page, T. F. *J. Mater. Sci.* **1985**, *20*, 4624−4646.
(9) Otte, K.; Lippold, G.; Frost, F.; Schindler, A.; Bigl, F.; Yakushev, M. V.; Tomlinson, R. D. *J. Vac. Sci. Technol., A* **1999**, *17*, 19−25.
(10) Belyansky, M.; Klymko, N.; Madan, A.; Mallikarjunan, A.; Li, Y.; Chakravarti, A.; Deshpande, S.; Domenicucci, A.; Bedell, S.; Adams, E.; Coffin, J.; Tai, L.; Sun, S.-P.; Widodo, J.; Lai, C.-W. *Mater. Res. Soc. Symp. Proc.* **2005**, *863*, 97−102.
(11) Ibach, H. *Surf. Sci. Rep.* **1997**, *29*, 193−263.
(12) Green, D. L.; Hu, E. L.; Stoffel, N. G. *J. Vac. Sci. Technol., B* **1994**, *12*, 3311−3316.
(13) Chen, C.-H.; Green, D. L.; Hu, E. L. *Appl. Phys. Lett.* **1996**, *69*, 58−60.
(14) Rahman, M. *J. Appl. Phys.* **1997**, *82* 2215−2224.
(15) Moulin, A. M.; O'shea, S. J.; Welland, M. E. *Ultramicroscopy* **2000**, *82*, 23−31.
(16) Ito, T.; Kato, I.; Nozaki, T.; Nakamura, T.; Ishikawa, H. *Appl. Phys. Lett.* **1981**, *38*, 370−372.
(17) Wong, S. S.; Oldham, W. G. *IEEE Electron Device Lett.* **1984**, *EDL-5*, 175−177.
(18) Kobeda, E.; Irene, E. A. *J. Vac. Sci. Technol., B* **1988**, *6*, 574−578.
(19) Itakura, A. N.; Narushima, T.; Kitajima, M.; Teraishi, K.; Yamada, A.; Miyamoto, A. *Appl. Surf. Sci.* **2000**, *159−160*, 62−66.
(20) Grunling, U.; Gujrathi, S. C.; Poulin, S.; Diawara, Y.; Yelon, A. *J. Appl. Phys.* **1994**, *75*, 8075−8079.
(21) Job, R.; Ulyashin, A. G.; Fahrner, W. R.; Ivanov, A. I.; Palmetshofer, L. *Appl. Phys. A* **2001**, *72*, 325−332.
(22) Wei, L.; Tabuki, Y.; Kondo, H.; Tanigawa, S.; Nagai, R.; Takeda, E. *J. Appl. Phys.* **1991**, *70*, 7543−7548.

NL071490X